2D sections of porosity and water saturation percent from combined resistivity and seismic surveys for hydrogeologic studies

R. MOTA, Laboratório Nacional de Engenharia Civil (LNEC), Lisboa, Portugal
F. MONTEIRO DOS SANTOS, Centro de Geofísica da Universidade de Lisboa, Portugal

Porosity and water saturation percent, or their product—the water content—are important parameters for most hydrogeologic studies. Geophysical methods, especially the resistivity method, are routinely applied to studying variations in these parameters at field scales. Resistivity is highly influenced by the presence of water in pore spaces and therefore well suited for studying fluids and saturation.

Laboratory and field work are being correlated to improve the understanding of relationships between geophysical measurements and soil physical and hydrologic properties. Resistivity and seismic methods have been combined to study the relationship between resistivity, seismic velocity, porosity, and water saturation. Recently, resistivity methods and ground-penetrating radar have been used independently to estimate water content and porosity.

Interpretation of geophysical data involves the resolution of the inverse problem, i.e., the determination of a model for the subsoil properties that fits the field data. In general it is possible to obtain more than one model that fits the data within satisfactory limits. In resistivity modeling this fact is known as the *principle of equivalence*. Seismic models are also nonunique. This is leading to joint application of different techniques in geophysical prospecting.

This study presents an approach for estimating porosity and water saturation percent by combining resistivity and seismic velocity data. We present a stochastic method of obtaining 2D sections for porosity and water saturation percent that combines 2D independent inversion of seismic and resistivity surveys. The method uses empirical laws relating seismic velocity and electrical resistivity with porosity, water content, and other parameters.

Several parameters such as water resistivity, clay resistivity, water velocity, clay velocity, air velocity, matrix velocity, clay percentage, and Archie's parameters are considered constant in the process. The values considered for each parameter come from literature and laboratory measurements.

Results from a test where field and laboratory measurements of void ratio and water content help to realistically evaluate the results.

The method. First, the two data sets are independently inverted; i.e., resistivity and P-wave refraction, using the same partition (cells) of the subsurface. This can be accomplished using commercial software: Res2DInv, for resistivity data, and Rayfract, for P-wave data. The results of separate inversions are the input data of an iterative process, which is performed in order to estimate the porosity and water content of the subsurface geologic formations. The method uses an expression derived from the empirical Archie's law for unsaturated material that accounts for the surface conduction effect, and a relationship between porosity, water saturation, and seismic velocity derived by Carrara et al. and based on Wyllie's mean velocity equation.

Electrical conductivity is mainly controlled by the ions present in the electrolyte total or partially filling the pore spaces. Conduction along grain surfaces (cation exchange) also has an important role, especially in fine-grain particles. A model based on the Hanai-Bruggeman equation relates electrical properties of a heterogeneous mixture to the properties of the

Box 1. *Resistivity and velocity relations and the objective function.*

The calculated resistivity is given by the modified Archie's law:

$$\rho_{cal} = \frac{a\,\rho_w\,\rho_{cl}}{a\,\rho_w\left(1-\phi^m\right)+\rho_{cl}\,\phi^m S_w{}^n} \qquad (1)$$

where ρ_{cal}, ρ_{cl}, and ρ_w stand for the effective, clay, and water resistivity, respectively; S_w is the water saturation degree; ϕ is the porosity, a is an arbitrary constant, and m and n are empirical parameters named *cementation factor* and *saturation exponent*, respectively.

The calculated velocity is given by Carrara's relation:

$$v_{cal} = \frac{1}{\dfrac{(1-\phi)(1-P_{cl})}{v_m}+\dfrac{(1-\phi)P_{cl}}{v_{cl}}+\dfrac{S_w\,\phi}{v_w}+\dfrac{\phi(1-S_w)}{v_a}} \qquad (2)$$

where P_{cl} is clay percentage and v_m, v_{cl}, v_w, and v_a are velocities for matrix, clay, water, and air, respectively. In this expression the terms with (1-ϕ) account for the mineral phase and the terms with ϕ are related with the pore-filling phase (air or fluid).

The SA objective function is defined by:

$$E = \alpha\sqrt{\frac{\sum_1^N\left(\dfrac{\rho_{obs}-\rho_{cal}}{\rho_{obs}}\right)^2}{N}} + \beta\sqrt{\frac{\sum_1^N\left(\dfrac{V_{obs}-V_{cal}}{V_{obs}}\right)^2}{N}} \qquad (3)$$

where ρ_{obs} and V_{obs} are resistivity and velocity from the independent inversion, ρ_{cal} and V_{cal}, are calculated from the iterative process, N is the number of points in the section, and α and β are constant weighting values ($\alpha + \beta$ =1.0).

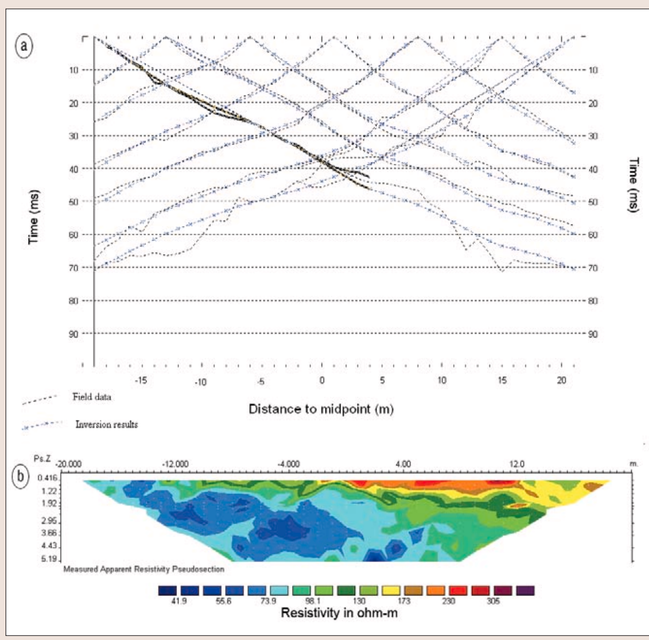

Figure 1. *(a) Field and inverted time-distance curves. (b) Field apparent resistivity pseudosection.*

individual components, accounting for conduction due to the brine and to the grain surface. Based on analysis of several different samples of clay, resistivity reduces as the dimension of soil particles gets smaller due to a larger conducting surface.

Here we present a similar approach, adding a term to Archie's law that represents the surface conduction due to the fine grain particles (equation 1 in Box 1).

The simulated annealing (SA) method was used for the iterative procedure. Each iteration is composed of several attempts. In each attempt the saturation (S_w) and the porosity (ϕ) are changed randomly, and their new values are unconditionally accepted if a decrease of the objective function E (equation 3 in Box 1) is observed. If E increases, the acceptance of the new parameter depends on the value of the function $P = exp(-\Delta E/T)$, where ΔE is the change in the objective function and T the "cooling temperature" that is compared with a randomly generated number Q between 0 and 1. The new parameters are only accepted if $P>Q$.

The annealing schedule needs a cooling temperature scheme to freeze the solution in the vicinity of the absolute minimum. Here we use a proportional cooling schedule—$T_i = 0.9\, T_{i-1}$—where i is the iteration number, with 1.02 selected for the initial value of temperature.

During the iterative process, resistivity and seismic velocity for air, matrix, water, and clay were imposed as constants. Matrix velocity at each cell is the mean value of the range where the velocity of the corresponding cell falls in the seismic refraction model (Table 1).

Table 1. *Values considered for matrix velocity (V_m); values for V_p are adapted from literature.*

Material	V_p (m/s)	V_m (m/s)
Loose soils	180–750	465
Clay and wet marl	750–1200	975
Sand and compact soils	1200–2400	1800
Sandstone	2400–3000	2700
Limestone and granite	3000–6000	4500
Gabbro and basalt	6000–7000	6500
Dunite	7000–9000	8000

Application of the method. A field test was performed at LNEC (Laboratório Nacional de Engenharia Civil) campus in Lisboa with a near-surface geology composed mainly of sand and gravel.

In February 2005, after a very dry winter season, a fresh soil sample was collected at a depth of 1.3 m at coordinate –1.0 (Figure 1), for laboratory determination of grain size distribution, water content (w), and void ratio (e). A surface moisture-density gauge (model 3440 from Troxler) was used to obtain in-situ values of water content and void ratio at four different levels—0.0, 0.1, 0.2, and 0.3 m—below ground-surface level immediately after excavation (Table 2).

P-wave refraction profiles were recorded with a 24-channel Bison 9000 seismograph. The energy source was an 11-kg hammer. Geophone spacing was 1 m, designed to match the resistivity survey. Data were recorded from two overlapping receiver spreads, each with 24 geophones, to allow construction of a 41-geophone gather—the same number of receivers

Table 2. *Soil samples laboratorial tests and in-situ results.*

Depth (m)	Grain size distribution (%) Silt < 0.074 mm	Sand 0.074-2 mm	Gravel > 2 mm	e lab	e field	$\phi^{(*)}$ lab (%)	$\phi^{(*)}$ field (%)	w lab (%)	w field (%)	$Sw^{(**)}$ lab (%)	$Sw^{(**)}$ field (%)
1.30	26.8	68.0	5.2	0.380	0.494	27.5	33.1	8.8	7.8	30.1	23.6
1.40	-	-	-	-	0.425	-	29.8	-	7.6	-	25.5
1.50	-	-	-	-	0.476	-	32.2	-	7.8	-	24.2
1.60	-	-	-	-	0.496	-	33.2	-	7.9	-	23.8

(*) – *porosity was calculated from void ratio values, with* $e = \frac{\phi}{1-\phi}$.

(**) – *water-saturation degree was calculated from water content and porosity values, using* $w = \phi S_w$.

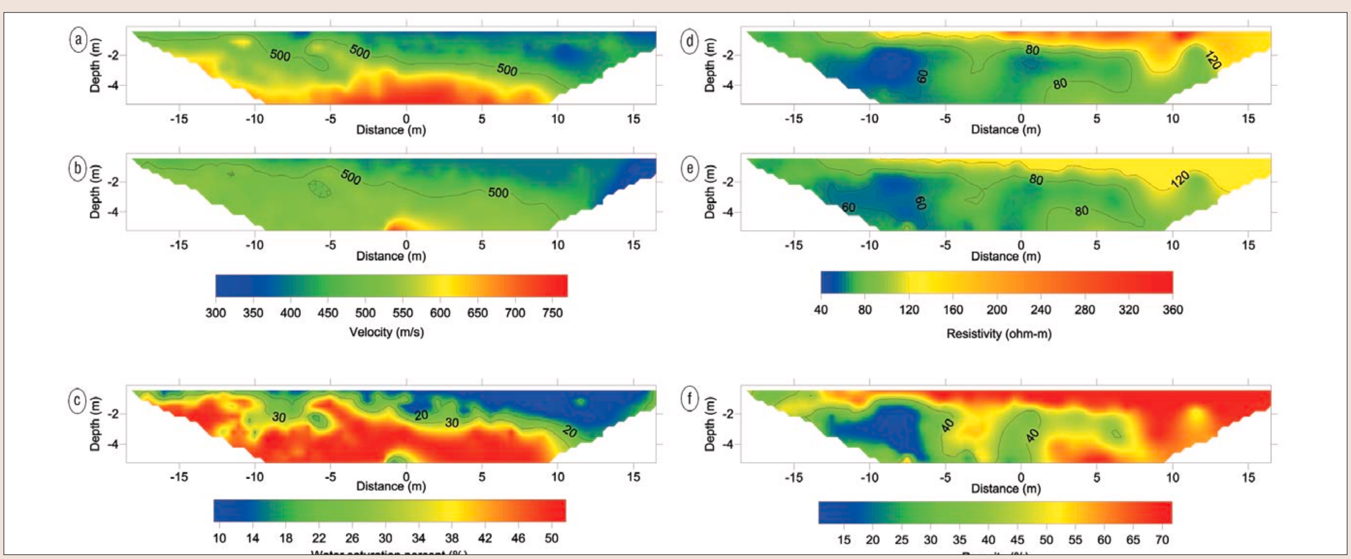

Figure 2. *(a) P-wave model from Rayfract. (b) P-wave from SA. (c) Water saturation percent, from SA. (d) Resistivity model from Res2DInv. (e) Resistivity from SA. (f) Porosity from SA.*

Table 3. *Parameters used in the SA best solution.*

ρ_w (ohm-m)	ρ_{cl} (ohm-m)	v_w (m/s)	v_{cl} (m/s)	v_a (m/s)	P_{cl} %	a	m	n	α	β
70	55	1 690	2 000	330	15	1.2	1.5	2	0.4	0.6

as resistivity electrodes.

Resistivity survey was performed with an ABEM LUND imaging system, using a Wenner array with dipole distances of 1 m.

Results. Data from seismic and resistivity surveys are presented in Figure 1. From time-distance curves it is possible to see that the soil is relatively homogeneous with a slight velocity increase with depth.

The models obtained from field data inversion with Rayfract and Res2DInv are presented in Figure 2 (relative misfit function in the inversion of seismic section: 1.480 ms; rms in resistivity: 5.1% after four iterations). From the observation of both results it is possible to see that the low velocity zone corresponds somehow to the higher resistivity top zone, which is an indication of low water content.

For the SA process several values of ρ_w and ρ_{cl} have been used in combination with different values of the Archie's parameters *a* and *m*. From those experiments it was possible to verify that changes in ρ_w and ρ_{cl} are more important than changes in Archie's parameters.

The best models obtained are presented in Figure 2. SA results were obtained after 120 iterations with almost 27 million parameter changes and an *E* final value of 16.6 (Table 3).

Analysis of independent inversion and SA results for 2D resistivity and seismic velocity sections suggests that both have a generally good match. Water saturation percent and porosity sections are in good agreement with values from field and laboratory tests (Table 2). Low resistivity and porosity values, generally between -7 m and -13 m, are probably due to the presence of finer soil particles.

Conclusions. The combined use of resistivity and seismic refraction methods yields porosity and water saturation degrees similar to those obtained from laboratory and field samples. Better results can be obtained if resistivity data from water samples and clay are available to eliminate part of the ambiguity present in the initial parameters used in the simulated annealing process.

Suggested reading. "Monte Carlo analysis of inverse problems" by Mosegaard and Sambridge (*Inverse Problems*, 2002). *Electrical Methods in Geophysical Prospecting* by Keller and Frischknecht (Pergamon Press, 1981). *Fundamentals of Soil Behavior* by Mitchell and Soga (John Wiley and Sons, 2005). "Geoelectrical and seismic prospection in hydrogeology: Model and master curves for the evaluation of porosity and water saturation" by Carrara et al. (*Pure and Applied Geophysics*, 1994). TLE

Acknowledgments: The authors express their appreciation to LNEC for fieldwork support. We thank Rick Miller for useful comments and suggestions that improved the final version of the manuscript.

Corresponding author: rmota@lnec.pt; rpmota@fc.ul.pt